

Study of Iron Impurity in Silver Chloride Using Mainly the Mössbauer Effect*

D. H. LINDLEY AND P. G. DEBRUNNER

Materials Research Laboratory and Department of Physics, University of Illinois, Urbana, Illinois

(Received 20 January 1966)

The Mössbauer effect has been investigated as a function of temperature between 4 and 550°K for sources of Co^{57} impurity diffused into single-crystal silver chloride. Auxiliary measurements of ionic conductivity, optical absorption, ESR, and dielectric dispersion have also been made. The Mössbauer spectrum of a freshly prepared sample is attributed to a ferrous ion in a substitutional site bound to a positive ion vacancy in a unique (100) position. Between 4 and 230°K a simple quadrupole doublet is observed which is interpreted to show a measure of covalency in the ferrous ion. Above 230°K the spectral lines broaden and the spectrum collapses to a single line; it is proposed that this effect is a result of the thermal motion of the vacancy around the impurity. The deduced vacancy jump times are shown to agree with those derived from dielectric-dispersion measurements. Aged samples have complex Mössbauer spectra which are explained by the formation of additional centers of ferrous ions bound to anion impurities.

I. INTRODUCTION

WE have employed the Mössbauer effect to study the properties of an iron impurity diffused initially as Co^{57} into single-crystal silver chloride. The Mössbauer spectra appear to represent two types of centers, one consisting of a ferrous ion associated with a silver-ion vacancy, and a second which is probably a divalent-anion impurity bound to a ferrous ion. A consistent interpretation of the spectra of the first type of center is developed which is based on additional information obtained from ESR measurements on Co^{2+} in AgCl and from dielectric-dispersion and ionic-conductivity measurements on cobalt- and iron-doped samples. It is shown that the Mössbauer effect is capable of giving information concerning the thermal motion of the silver-ion vacancy around the Fe^{++} ion.

The properties of some transition-ion impurities in the alkali and silver halides have been studied by the techniques of ESR, ENDOR and optical absorption. A classic work is that of Watkins,¹ who used ESR and dielectric dispersion to examine divalent manganese in the alkali chlorides. He found that the manganese was present substitutionally as Mn^{++} in an alkali-metal atomic site and that at low temperatures a charge-compensating cation vacancy was present either in a nearest-neighbor (110) or next-nearest-neighbor (100) position. At temperatures above 200°C the spin-resonance lines became broadened by the thermal motion of the vacancies around the impurities. Watkins showed that the atomic jump times estimated from ESR were consistent with those calculated from the measured frequencies of dielectric dispersion arising from the finite orientation times of vacancy-impurity dipoles. In a similar spin-resonance experiment in silver chloride Daehler² has shown that Mn^{++} ions at 77°K have vacancies bound in the next nearest neighbor (100) position only. The vacancy jump times are much

shorter than for the alkali halides, and line broadening is observed at 270°K instead of 500°K. The properties of ferrous impurities in silver chloride are expected to be similar to those of the other divalent transition metal ions. Since spin-resonance is not feasible for this system³ the Mössbauer technique is the most adequate method for studying Fe^{++} in silver chloride.⁴ The Mössbauer effect of the 14-keV transition of Fe^{57} provides a convenient way of measuring the hyperfine fields acting on the iron nucleus and in addition it yields information about the root-mean-square displacement of the impurity atom in the host lattice.

By suitable source preparation it has been possible to obtain samples containing cobalt-vacancy pairs only. Between 4° and 230°K, the Mössbauer spectra from these crystals consist of a simple quadrupole doublet whose splitting has the expected temperature dependence.⁵ A variety of evidence (Secs. V and VII) shows that the cobalt ion is substituted for a silver ion, with the cation vacancy apparently in a unique site which, from the ESR work of Sliker⁶ on Co^{++} in AgCl , we deduce to be next nearest neighbor (100). Using this symmetry for the crystalline-field distortion it is found that significant covalency corrections have to be made in order to fit theory with experiment.

As the temperature is raised above 230°K the spectral shape changes; the temperature dependence of the splitting becomes anomalously large and the lines

³ W. Hayes, J. R. Pilbrow, and L. M. Slifkins, *J. Phys. Chem. Solids* **25**, 1417 (1964).

⁴ It should be noted that in our experiment we study the decay product Fe^{57} of the radioactive Co^{57} impurity. The energy levels of the 14.4-keV state of Fe^{57} are measured as they exist for a time interval of the order of 10^{-7} sec after K capture. It is not known *a priori* whether the newly formed iron ion will remain in the lattice site of the parent Co^{57} ion. From lack of evidence to the contrary it is assumed that the Co^{57} and Fe^{57} do indeed occupy identical positions. This is supported by ionic conductivity data which indicates that iron in AgCl is normally in a substitutional site. It is also noted that there is no evidence even at 4°K of the anomalous charge states of Fe^{57} which have been observed in certain other ionic crystals [R. L. Ingalls and G. de Pasquali, *Phys. Letters* **15**, 262 (1965)]. We conclude that the lifetimes of these states are shorter than 10^{-7} sec.

⁵ R. L. Ingalls, *Phys. Rev.* **133**, A787 (1964).

⁶ T. R. Sliker, *Phys. Rev.* **130**, 1749 (1963).

* Supported by the U.S. Atomic Energy Commission under Contract AT(11-1)-1198 and U. S. Navy Contract ONR 1834(05).

¹ G. D. Watkins, *Phys. Rev.* **113**, 79 (1959); **113**, 91 (1959).

² M. Daehler, Ph.D. thesis, University of Wisconsin, 1963 (unpublished).

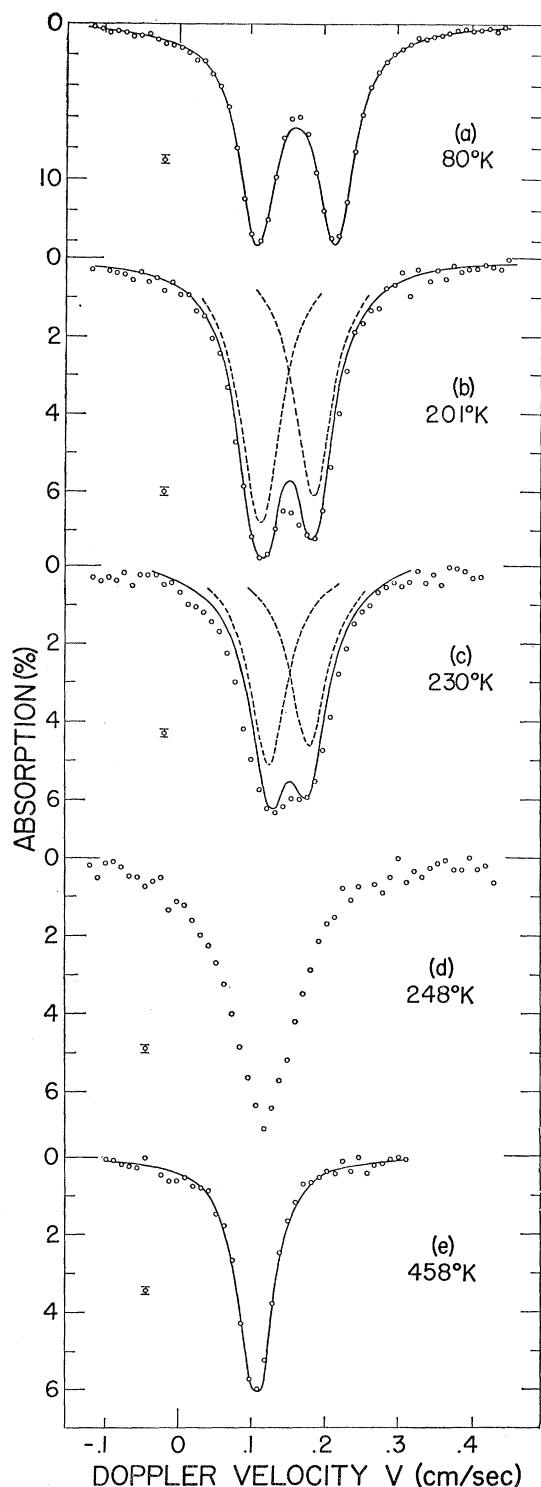


FIG. 1. Mössbauer spectra for a freshly prepared sample of Co^{57} in AgCl at five temperatures. The absorber was enriched stainless steel. The solid lines in (a), (b), and (c) are two line spectra whose components are Lorentzian and have widths 0.06 cm/sec. The single line in 1(e) is a Lorentzian of width 0.059 cm/sec. Positive Doppler velocity represents motion of the absorber away from the source.

broaden. This unexpected behavior is attributed to the time-dependent fluctuation of the field gradient caused by the motion of the vacancy. The estimated vacancy jump times agree within an order of magnitude with those found by Daehler² and with those derived from our measurements of dielectric dispersion in both iron and cobalt-doped samples.

Spectral broadening at 230°K, similar to that in AgCl , is also observed for Co^{57} in AgBr single crystals.

If the samples are left for some time at room temperature, the second type of center begins to form and the Fe^{++} -vacancy spectrum is partially replaced by a spectrum which is believed to represent an anion impurity bound to the Fe^{++} ion. In one sample we have definite evidence that the impurity is oxygen. This phenomenon is analogous to the behavior of the $\text{AgCl}:\text{Mn}^{++}$ system.² We have not studied these centers in detail but have demonstrated that they dissociate above 100°C and that they possess a quadrupole splitting with an anomalous temperature dependence.

II. APPARATUS AND EXPERIMENTAL PROCEDURE

The samples were prepared from single crystal silver chloride slabs of approximate dimensions $0.5 \times 0.5 \times 0.2$ cm cut mostly from material obtained from the Harshaw Chemical Company. These slabs were etched in hypo to remove damaged material, washed with distilled water and then hydrochloric acid. A drop of 4*N* HCl containing the active Co^{57} was then placed on the surface and allowed to evaporate. Heating for 6 h at 370°K in a mixture of 95% argon and 5% chlorine ensured that the cobalt diffused between 10^{-1} and 10^{-2} cm into the bulk of the solid. Finally, the samples were etched in hypo and rinsed in distilled water. The first specimens were handled under safelights but experiment showed this to be unnecessary and this precaution was later discarded.

The auxiliary measurements of ionic conductivity, dielectric dispersion, optical absorption and ESR were made with samples doped with inactive cobalt by a procedure similar to that described above. These specimens were however heated for long periods, typically 70 h at 420°C, to ensure a uniform distribution of impurity. Crystals containing iron were also examined and these were either cut from a boule which had been doped in the melt or prepared by a method due to Sliker.⁷ This consists of placing iron filings on the surface and heating in the argon-chlorine atmosphere for about $\frac{1}{2}$ h at 400°C. Surplus filings are then removed by washing with HCl and the sample is given the prolonged heat treatment.

The impurity concentration in these samples as determined by emission analysis⁸ was in the range 100

⁷ T. R. Sliker, Ph.D. thesis, Cornell University, 1962 (unpublished).

⁸ Undertaken by Anderson Laboratories, Champaign, Illinois.

to 1000 ppm. The estimated average concentration of Co^{57} nuclei within one diffusion length from the surface of the Mössbauer specimens also lies in this range.

Two samples of Fe^{57} in silver bromide were fabricated by a technique similar to the one described for the chloride. HBr was used instead of HCl both in rinsing and as a solvent for the cobalt. The diffusion was performed for 6 h at 400°C in a flow of nitrogen which had been bubbled through liquid bromine.⁹

Mössbauer spectra were obtained against an Fe^{57} -enriched stainless-steel absorber driven in sawtooth motion by a University 8 CHC loudspeaker. The drive and pick-up unit was essentially that described by Wertheim.¹⁰ An RIDL 400-channel analyzer used in the analog mode stored the pulses. Calibration spectra were taken with a source of Co^{57} in iron.

The temperature of the sample could be held at 4.2°K or at a value between liquid-nitrogen and room temperature. A water-cooled evacuated oven enabled spectra to be taken between 300 and 550°K . The fluctuations in temperature were generally less than 0.5°K .

III. MÖSSBAUER RESULTS

The observed spectra can be conveniently grouped into two classes, namely those derived from freshly prepared samples and those from samples which had remained at room temperature for times ranging from a few days to several weeks. The former class of spectra is labeled I and clearly represents ferrous ions in a unique environment. The latter category, less well defined and sample dependent, consists of highly complex spectra which are made up of spectrum I and two other components which we label II and III, respectively.

A. Spectrum I

Figure 1 shows typical type I spectra for (a) 80°K , (b) 201°K , (c) 230°K , (d) 248°K , (e) 458°K . The results were completely reproducible, were independent of sample with one exception discussed below, and independent of the time taken to reach the particular temperature of measurement. The concentration of cobalt introduced into the crystal was varied by a factor greater than 20 through addition of inactive cobalt to the Co^{57} solution in HCl. No effect was observed. The data were analyzed in terms of lines of Lorentzian shape fitted by a least-squares computer program.¹¹ The solid curve drawn in Fig. 1 (a) shows the fit obtained at these temperatures to two lines of nearly equal intensity and of equal width of value 0.06 ± 0.002 cm/sec. The spectrum at 4.2°K is similar

⁹ Argon and hydrogen bromide atmospheres were also tried but the cobalt remained on the surface of the crystal.

¹⁰ G. K. Wertheim, T. M. C. Corp., Technical Application Bulletin No. 1, North Haven, Connecticut (unpublished).

¹¹ J. Burton, Ph.D. thesis, University of Illinois, 1965 (unpublished).

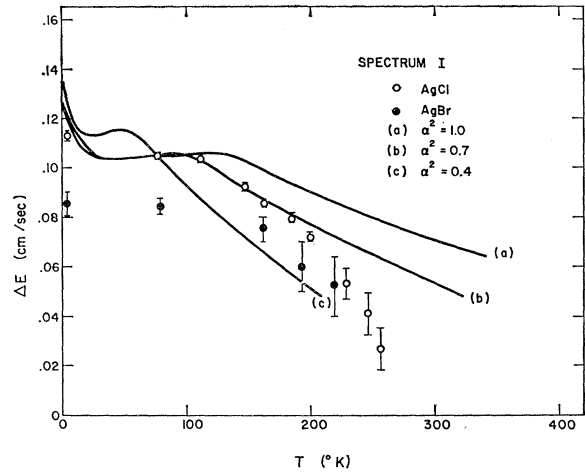


FIG. 2. Quadrupole splitting ΔE versus temperature for spectrum I. The open circles are Co^{57} in silver chloride, the closed circles cobalt in silver bromide. The theoretical curves are arranged to pass through the AgCl experimental point at 80°K and are for the following parameters $\lambda_F = 100$ cm^{-1} , (a) $\alpha^2 = 1.0$, $\Delta_F = 100$ cm^{-1} , (b) $\alpha^2 = 0.7$, $\Delta_F = 100$ cm^{-1} , (c) $\alpha^2 = 0.4$, $\Delta_F = 125$ cm^{-1} .

to that at 80°K but slightly broader (0.067 cm/sec) because of vibration in the cryostat. The width at 80°K is the same as that obtained for a magnetically split cobalt-in-iron source against the same absorber.

As the temperature is raised the splitting ΔE between the two lines [Fig. 1(a)] decreases until at about 240°K the two lines can no longer be resolved. The line width appears to increase slightly with temperature above 180°K but between 230 – 240°K the character of the spectrum changes; the lines broaden by about 50% and, if the two widths are constrained in the fit to be equal, the intensity of the line nearer zero velocity is typically twice that of the other. A better fit is achieved by allowing the widths of the doublet to differ. It is then found that the line nearer zero has 30–50% greater width than the other and the ratio of the areas is larger than two. At higher temperatures the resolved two-line character is lost and a broad almost symmetrical line is observed of typical width 0.1 cm/sec at 250°K (e.g. Fig. 1(d)). Above 270 – 280°K this single line narrows until at about 320°K it has the width of the 80°K spectrum, i.e., 0.06 cm/sec (e.g. (Fig. 1(e)). To illustrate these changes in line width spectra made up of lines with width 0.06 cm/sec are drawn-in in Figs. 1(b) and (c). The areas chosen for the components are nearly equal since this is what one would expect from the unambiguous lower temperature data.

Above 320°K the single line, narrow width character is retained up to the highest experimental temperatures, namely 550°K . The width of the Lorentzian drawn in Fig. 1(e) for instance is 0.059 cm/sec.

Figure 2 is a plot of quadrupole splitting ΔE versus temperature derived from spectra such as those in Fig. 1. Points are included up to 250°K . The large error bars on points between 200 and 250°K express the uncer-

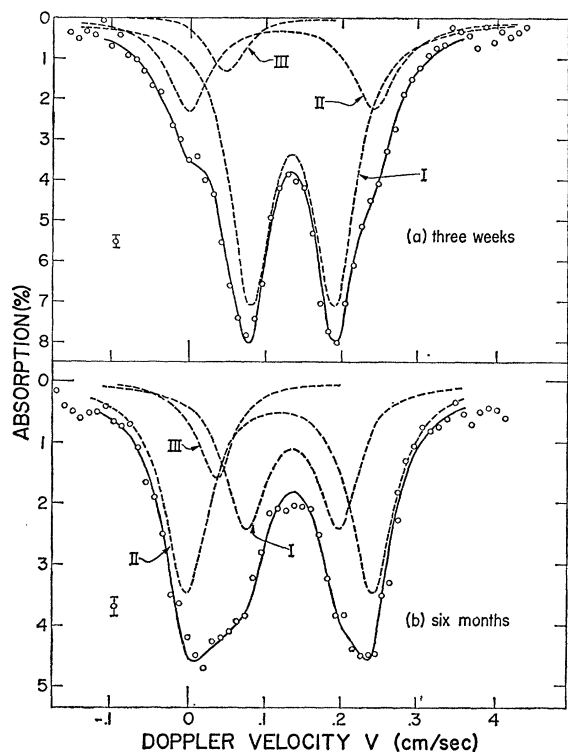


FIG. 3. Mössbauer spectra taken at 80°K of two samples AgCl:Co⁵⁷ stored at room temperature for (a) three weeks and (b) six months. The dashed curves show the analysis of the spectra. The doublets labeled I have the splitting and widths of the spectrum in Fig. 1(a). The full line is the sum of the intensities of the dashed.

tainty wrought in this region by the anomalous spectral shapes.

The samples of silver bromide showed similar behavior to silver chloride but with slightly smaller ΔE : These splittings are also plotted in Fig. 2. The changes in line shape were not examined closely but qualitatively these appeared similar to the AgCl system.

B. Spectra II and III

After the sample has been kept a few days at room temperature extra lines appear. Measurements at 80°K where the recoilless fractions are large and the spectrum I lines are narrow show that a quadrupole-split spectrum of ΔE approximately twice that of I grows at the expense of the intensity of I. Apparently the center associated with the latter converts to a center of different properties. Figure 3 shows spectra from a sample stored at room temperature for (a) three weeks and (b) six months. The rate of conversion is dependent on the sample temperature since spectrum II does not appear in crystals kept at liquid nitrogen temperatures. Both I and II are unaffected by uv irradiation even though the sample is black with precipitated silver. Annealing in the chlorine-argon atmosphere (or in air or vacuum) for a few minutes at 400°C or a few hours at 100°C is

however sufficient to reconvert II back completely to I.

Using the computer program to subtract the spectrum I lines of known position and width from the composite spectra it is found that the character of spectrum II is sample dependent. In fact, it can change with time for one sample and seems to get more complex as its intensity increases. The splitting ΔE at 80°K can lie anywhere between 0.21 and 0.25 cm/sec and the widths between 0.07 and 0.08 cm/sec. In addition, there is often a third line present (III) at about +0.04 cm/sec with a width 0.05–0.08 cm/sec. This line appears to be associated with a precipitated phase since it is especially strong in very old samples and in samples which have been stressed. The dashed lines in Fig. 3 show the computer analyses of these spectra.

A unique specimen was a crystal cut from a boule which had been grown from a melt through which wet oxygen had been passed. The 80°K spectrum obtained immediately after preparation showed the intensity of spectrum I to be much reduced and the spectra dominated by well defined quadrupole split lines of fairly narrow width (0.067 ± 0.002 cm/sec) but possessing a rather large ΔE (0.24 ± 0.005 cm/sec). This spectrum and its analysis is shown in Fig. 4.

Figure 5 shows ΔE versus T for the latter sample and the sample of Fig. 3(b). These data illustrate the differences between samples.

C. Recoilless Fraction f and Isomer Shift δE

Figure 6 shows the logarithm of recoilless fraction f versus temperature plotted for (i) spectrum I between 4 and 530°K (closed circles), (ii) spectrum II, specimen of Fig. 3(b) between 4°K and room temperature (triangles), and (iii) spectrum II of the oxygen-doped sample (open circles). This latter crystal gave f 's which were higher than those of other spectra II.

The spectrum I values were calculated from the areas of Fig. 1, the known f of stainless steel at room temperature¹² and a measured background correction. The f for spectrum II was calibrated in magnitude relative to spectrum I by observing the change in area which occurred when a complex spectrum such as that of Fig. 3(b) was converted to a simple pure spectrum I by a rapid heat treatment. The f 's for the oxygen sample are, therefore, relatively inaccurate since, in this case, no such conversion could be made.

The difference in the intensities of the two components of spectrum I between 140 and 230°K (e.g., Figs. 1(b), 1(c)) is attributable to a root-mean-square displacement of the Fe⁵⁷ nucleus which is anisotropic.¹³ The range of temperatures where the two intensities can be sensibly separated is small so average f 's are quoted in Fig. 6. Spectrum II shows evidence of the effect but the complexity of the spectrum makes the results uncertain.

¹² P. G. Debrunner and R. J. Morrison, Rev. Mod. Phys. 36, 463 (1964).

¹³ W. J. Nicholson and G. Burns, Phys. Rev. 129, 2490 (1963).

FIG. 4. Mössbauer spectrum at 80°K for an AgCl:Co⁵⁷ sample which was prepared from an AgCl crystal doped with oxygen during growth. The solid line is the computer analysis composed of the dashed line components: the inner doublet marked I has the splitting and linewidth of spectrum I at 80°K, i.e., that of Fig. 1(a).

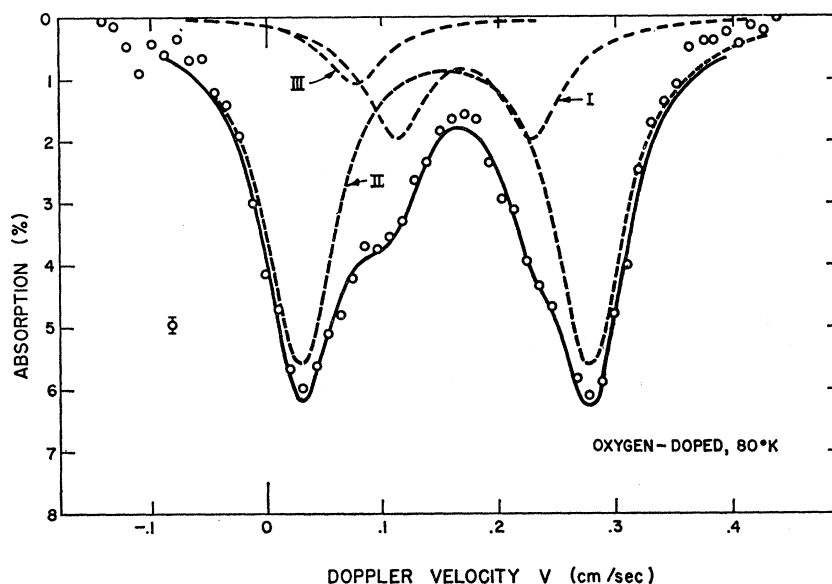


Figure 7 gives the isomer shift δE relative to Fe⁵⁷ in iron plotted as a function of temperature for both spectra I and II.

IV. MODEL FOR SPECTRUM I

We propose that the low-temperature (<200°K) spectra I are characteristic of a ferrous ion substituted for a silver ion with a cation vacancy in a next nearest neighbor (100) site.

It appears certain that the iron is present in the doubly charged state since the room-temperature

isomer shift is large (0.106 ± 0.005 cm/sec) compared to what one would expect for the trivalent state (~ 0.04 cm/sec).¹⁴ However, the former value is quite

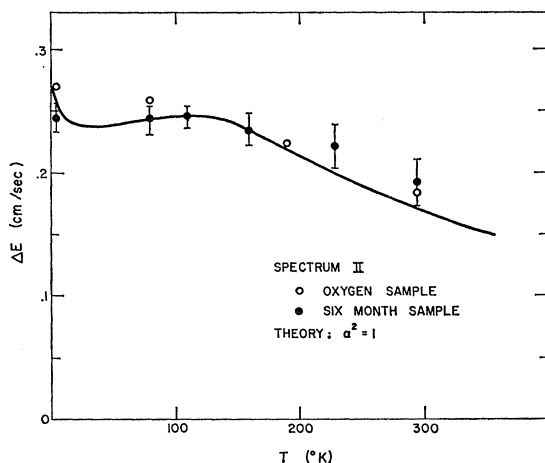


FIG. 5. Quadrupole splitting ΔE versus temperature for the oxygen-doped sample of Fig. 4 (open circles) and the six-month-old sample of Fig. 4(b) (closed circles). The theoretical curve is arranged to pass through the closed circle point at 80°K and has the parameters $\Delta_F = 230$ cm⁻¹, $\lambda_F = 100$ cm⁻¹, $\alpha^2 = 1$. The error bars from the oxygen-doped sample have been omitted since no theory is fitted; the errors are comparable to the six-month sample.

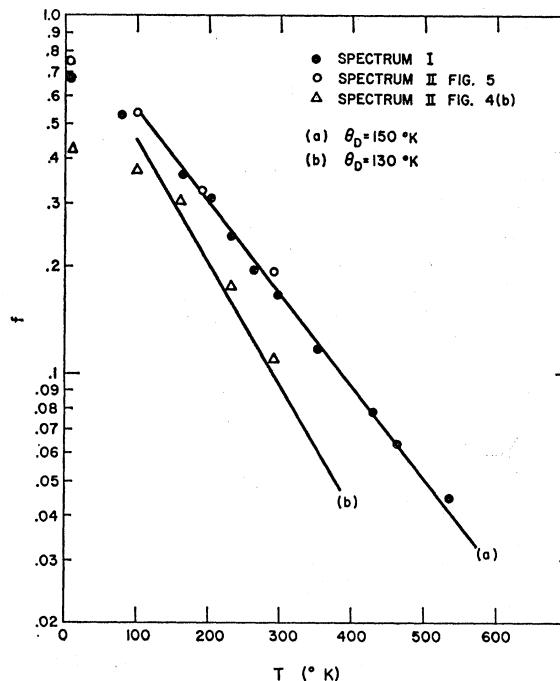


FIG. 6. Logarithm of recoilless fraction f against temperature. The closed circles are for spectrum I, the triangles for spectrum II. A unique set of values for f is that derived from the spectrum II of the oxygen-doped samples. Unlike the other spectra II these f 's are comparable to those of spectrum I. The straight lines represent a Debye model in the high-temperature limit ($T > \frac{1}{2}\Theta_D$) and are for Debye temperatures of (a) 150 degrees, (b) 130 degrees.

¹⁴ L. R. Walker, G. K. Wertheim, and V. Jaccarino, Phys. Rev. Letters 6, 98 (1961).

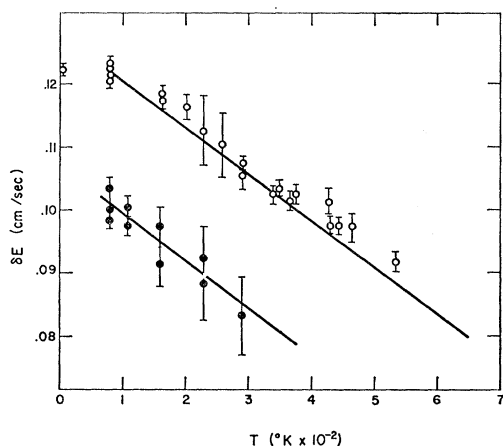


FIG. 7. Isomer shift δE , relative to a cobalt-in-iron source versus temperature. The open circles are for spectrum I, the closed for spectrum II (the oxygen-doped sample gives values close to those of other spectra II). The straight lines represent the changes predicted by the high-temperature limit ($T > \frac{1}{2}\Theta_D$) of a Debye model, i.e., they have a slope 7.3×10^{-5} cm/sec deg. The lines are shifted to pass through the respective experimental points at 80°K.

far from that attributed to a pure $3d^6$ divalent state, namely 0.125 cm/sec. A further argument in favor of Fe^{++} is that cobalt in AgCl is present only as Co^{++} . The evidence for this latter fact is strong and includes ESR, optical and conductivity data (see Sec. V(A) and VII).

The electric-field gradient (EFG) at the Fe^{++} nucleus and hence the quadrupole splitting arise from the distortion caused by the vacancy in an otherwise cubic crystalline field. This is consistent with the high-temperature single-line spectra which, in an ionic crystal, can arise only from effective cubic symmetry. It is assumed that at these temperatures the EFG due to the vacancy fluctuates in time so quickly that it averages to zero or that the vacancy has dissociated from the ion. The evidence for the presence of the vacancy is clear and includes the independence of the spectra from cobalt concentration and the failure to quench-in the high temperature line. The difficulty of quenching-in a divalent impurity isolated from a vacancy is a well known property of AgCl.^{3,6,15} The evidence for the position of the ion and of the vacancy is derived mainly from the work of Sliker⁶ on cobalt in AgCl⁶ and this is discussed in the next section. Information on ionic conductivity is also relevant (Sec. VII).

The broadening and change in spectral shape at 230°K and above are thought to be a result of the thermal motion of the vacancy. To confirm this we have made measurements of the dielectric dispersion (Sec. VI).

V. QUADRUPOLE SPLITTING AS A FUNCTION OF TEMPERATURE FOR SPECTRUM I

For axial symmetry the quadrupole splitting ΔE is directly proportional to the E.F.G. at the Fe^{37} nucleus,

¹⁵ R. F. Tucker, Phys. Rev. **112**, 725 (1958).

V_{zz} , by

$$\Delta E = \frac{1}{2} e Q V_{zz}.$$

Here e is the electron charge and Q the excited-state quadrupole moment.

The EFG at the ferrous ion nucleus is almost completely due to the charge distribution of the core and $3d$ electrons. However, although external charges (i.e., the lattice field) make a small contribution, this very field is needed to polarize the electrons on the ion to produce the EFG. Thus to determine the temperature dependence of the EFG it is essential to know the symmetry of the crystalline field. Since our ΔE temperature dependence proves to be anomalous we examine below the evidence for the nature of the Fe^{++} site.

A. The Co^{++} and Fe^{++} Sites

Doubly ionized transition impurities tend to occupy substitutional sites in silver chloride.^{2,3,15,16} Sliker⁶ has examined optical and ESR spectra of cobalt ions at low temperatures in AgCl. His measurements have been repeated in outline¹⁷ on samples whose preparation was described in Sec. II and it is concluded that cobalt is present in centers substantially identical with his.

Sliker interpreted his optical data with success in terms of a cubic crystalline field resulting from an octahedron of negative charges. However, the spectra cannot reveal the presence of a small noncubic distortion, nor, since the lines are so broad, can an interpretation be entirely satisfactory. The ESR measurements on the other hand are sensitive to the distortion and are unambiguous.

Sliker found that the majority of the ESR data could be attributed to a center which had (100) symmetry and spin-Hamiltonian parameters $g_{11} = 5.38$, $g_1 = 3.87$, $A = 233 \times 10^{-4}$ cm⁻¹, and $B = 89 \times 10^{-4}$ cm⁻¹. It can be demonstrated from the work of Abragam and Pryce,¹⁸ that these parameters imply that the crystal field arises from a regular octahedral configuration. In this environment the sevenfold degenerate orbital level splits into a low-lying triplet, a second triplet, and a high singlet. The ground-state Kramers doublet is essentially a mixture of the three states making up the low triplet. The mixture is a result of the perturbation from the non-cubic distortions and spin-orbit coupling. An axial distortion splits the low triplet into a singlet and doublet. If we write its perturbation in terms of this splitting Δ_c then it is found that to a good approximation g_{11} and g_1 are both functions of the single parameter Δ_c/λ_e , where λ_e is the spin-orbit coupling constant for a cobalt ion; g_{11} and g_1 thus bear a functional relationship to each other. It is found that the observed values of g do indeed satisfy this relationship; a plot of g_{11} versus

¹⁶ H. C. Abbink, Ph.D. thesis, Iowa State University, 1964 (unpublished).

¹⁷ We are indebted to Dr. B. Joesten for the optical measurements and to Professor H. Stapleton for the ESR measurements.

¹⁸ A. Abragam and M. H. L. Pryce, Proc. Roy. Soc. (London) **A205**, 135 (1951); **A206**, 173 (1951).

Δ_c/λ_c is shown in Fig. 8. This calculation of g_{II} entails simply a diagonalization of the matrix obtained from the aforementioned perturbation of the low-lying triplet basis states. From Fig. 8 it is seen that Δ_c/λ_c is about -2 from the measured g_{II} . Since λ_c for the free ion is negative it is certain that this is also true for the ion in the solid. This implies a positive value of Δ_c and is consistent with a distortion resulting from a negative charge (positive ion vacancy) on the z axis.

The self-consistency of this calculation can be checked by computing the hyperfine structure constants A and B from the amplitudes of the basis orbital states making up the ground state. We find $A=260 \times 10^{-4} \text{ cm}^{-1}$, $B=90 \times 10^{-4} \text{ cm}^{-1}$ which compares favorably with the experimental values. It is noted that we make use of the work of Abragam, Horowitz, and Pryce,¹⁹ who showed that the Fermi contact interaction is independent of the ion environment.

The evaluation of Sliker's data is therefore consistent in every way with a picture of the cobalt in a substitutional site and an effectively negatively charged vacancy lying in the $[100]$ direction. If the cobalt were in an interstitial site, then the resulting tetrahedral configuration would reverse the sign of the cubic component of the field. The singlet would then be low lying instead of the triplet. Both g values would be expected to be close to 2 in this case.²⁰

Daehler² has shown that Mn^{++} in AgCl is octahedrally coordinated with a distortion having a symmetry axis in the $[100]$ direction. The sign of D , the appropriate spin-Hamiltonian parameter, is negative as would be expected for the negative field of a cation vacancy.¹³

Although there seems little doubt that the cobalt is present substitutionally, this does not necessarily mean that Fe^{++} is also substitutional. It would, however, seem unlikely that the iron would jump into an interstitial position following K capture. We have attempted to determine the symmetry of the center using the anisotropy of the recoilless fraction f (Sec. IIIC). The angular dependence of the ratio of the intensities of the two low-temperature spectral lines in single crystals of known orientation could, with a few simplifying assumptions, give the orientation of the EFG with respect to the crystal axes, and hence the symmetry of the crystalline-field distortion. Unfortunately, the effect, if present, proved to be too small to detect.

From ionic conductivity measurements it does appear that iron behaves as if it associates with one silver ion vacancy as has already been noted by Hayes *et al.*³ If it were interstitial and doubly charged, it is expected that two vacancies would be involved.

B. Calculation of ΔE as a Function of Temperature

The Fe^{++} ion, if substitutional, will be surrounded by an octahedron of negative ions; Fig. 9 illustrates the

¹⁹ A. Abragam, J. Horowitz, and M. H. L. Pryce, Proc. Roy. Soc. (London) A230, 165 (1955).

²⁰ K. D. Bowers and J. Owen, Rept. Progr. Phys. 18, 304 (1955).

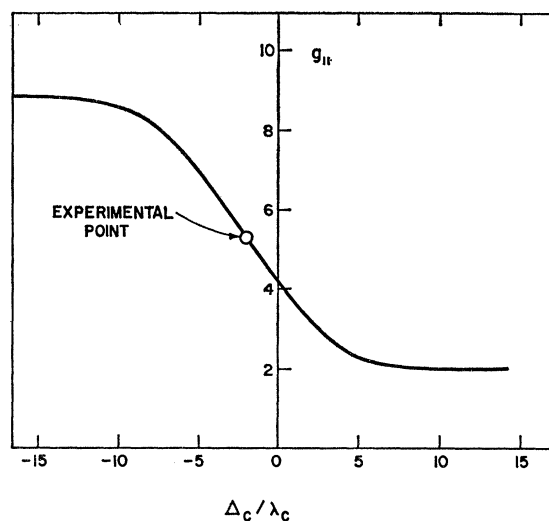


Fig. 8. Spin-Hamiltonian parameter g_{II} versus the ratio of the splitting factor Δ_c and spin-orbit coupling constant for cobalt λ_c .

expected energy-level scheme.⁵ The fivefold degeneracy of the 5D orbital state is lifted by the dominant cubic component of the crystal field to give a high doublet (d_γ) and low triplet (d_e). These degeneracies are further lifted by the axial distortion brought about by the presence of the vacancy.

In a simple point-ion model the distortion potential for a charge q , $2a$ from the origin on the z axis is

$$V_{\text{dist}} = \frac{qz}{4a^2} + \frac{q}{16a^3}(3z^2 - r^2)$$

+ cubic and higher order terms.

Terms of odd power in z can, however, be neglected since they imply a net force on the ion and, moreover, their matrix elements are zero for d -electron wave functions.²¹ Neglecting fourth-order terms, the distortion potential can thus be written in the usual axial form (Ref. 5)

$$V_{\text{dist}} = B_2^0(3z^2 - r^2).$$

B_2^0 is a constant which for the point-ion model is of the order $q/16a^3 \sim 2 \times 10^{-3}$ a.u. If q is negative V_{dist} separates the triplet into a ground singlet state, transforming as xy and a higher doublet (transforming as xz, yz) separated from $|xy\rangle$ by Δ_F , where

$$\Delta_F = (6/7)B_2^0\langle r^2 \rangle.$$

The EFG at the ferrous ion nucleus is primarily a result of the electron charge distribution corresponding to these three orbital levels. The temperature dependence of the EFG is due to the change in Boltzmann population of the levels.

²¹ B. Bleaney and K. W. H. Stevens, Rept. Progr. Phys. 16, 108 (1953).

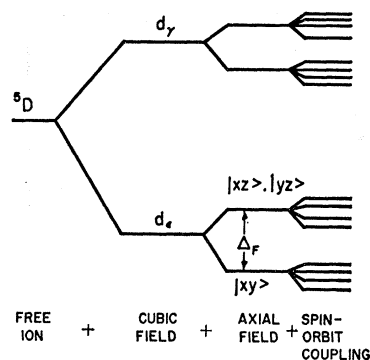


FIG. 9. The energy level scheme for the ferrous ion under the action of a crystalline field from Ref. 5.

V_{zz} for $|xy\rangle$ is $(4/7)\langle r^{-3} \rangle$ and $(-2/7)\langle r^{-3} \rangle$ for $|xz\rangle$ and for $|yz\rangle$. Thus, at low temperatures, where $|xy\rangle$ alone is populated, the EFG is positive, and as the temperature increases, it decreases smoothly until it becomes zero at temperatures $T > \Delta_F/k$. This is not surprising since it represents effective cubic symmetry. For an appreciable change in EFG over an interval ΔT , therefore, Δ_F must be of the order $k\Delta T$.

The effect of spin-orbit splitting is to lift the spin degeneracy ($2S+1=5$) of each orbital level and to couple $|xy\rangle$, $|yz\rangle$, and $|xz\rangle$. Each new level is therefore a mixture of all three of these states and gives a low temperature EFG much reduced in magnitude from $4/7\langle r^{-3} \rangle$. The variation with temperature is correspondingly flattened.

The three theoretical curves in Fig. 2 of ΔE versus T are for an axial distortion taking into account spin-orbit interaction. The curves were derived from calculated values similar to ones plotted in Fig. 3 of Ref. 5 and represent the expression

$$\Delta E = 0.54(\alpha^2)F(\Delta_F, \alpha^2\lambda_F, T) \text{ (cm/sec)}. \quad (\text{Eq. 42, Ref. 5})$$

Here λ_F is the free-ion spin-orbit coupling constant and α^2 the reduction factor, usually assumed to be 0.8, which takes into account covalency effects. F is a numerically evaluated function which incorporates both crystalline field distortion and spin-orbit effects.

The three curves have differing values of α^2 and almost the same value for Δ_F since the magnitude of F at its plateau (in the range 20–100°K) is a linear function of $\Delta_F/\alpha^2\lambda_F$ for $\Delta_F/\alpha^2\lambda_F \leq 3$. The parameters are adjusted so that the curves pass through the most accurately determined experimental point, namely that at 80°K. The best fit is evidently for $\alpha^2=0.7$, $\Delta_F=100 \text{ cm}^{-1}$. However, this fit is satisfactory below 200°K only; above this temperature the experimental points tend too rapidly to zero. We attribute this anomaly to the motion of the vacancy discussed in the next section.

The requirement that the spin-orbit coupling constant $\alpha^2\lambda_F$ needed to fit the data below 200°K be smaller than the free ion value $\lambda_F (=100 \text{ cm}^{-1})$ is independent of the assumed symmetry of distortion. This can be explained as follows: In order to obtain appreciable change of ΔE (EFG) in an interval ΔT , Δ_F must be of the order of

$k\Delta T$. However, λ_F is 100 cm^{-1} corresponding to a temperature interval of 150°K. The effect of spin-orbit coupling is to mix states of opposite sign in EFG and to spread out in energy the five spin-orbit levels originating from each orbital level. Thus any steep variation of ΔE with T resulting from a reduction in Δ_F is counteracted by the effects of $\alpha^2\lambda_F$. There is therefore a maximum slope to ΔE versus T for a given $\alpha^2\lambda_F$ and a given temperature range, as can readily be seen in Figs. 3, 4, and 5 of Ref. 5.

It is noted that the argument is dependent on the dominant cubic component of the crystalline field being a result of an octahedral configuration. If the ferrous ion were tetrahedrally coordinated as would happen for an interstitial site, then the sign of the field is reversed and the upper d_γ doublet of Fig. 9 becomes the lower lying levels. These d_γ orbitals are split by an axial or rhombic distortion but are *not* mixed by spin-orbit interaction. Hence a sharp temperature dependence of the EFG can be obtained by taking a splitting of the appropriate value.

VI. MOTION EFFECTS

As stated in the previous section the marked changes in spectral shape for spectrum I in the region 230–280°K are attributed to the time dependence of the EFG caused by the thermal motion of the vacancy around the Fe^{2+} ion. A detailed model for this effect is not available but analogies can be made with those Mössbauer relaxation effects already observed for fluctuating paramagnetic fields²² and with motional narrowing in NMR.²³

The limiting cases of slow and fast motion are easily defined and correlated with the observations. For slow motion the time-averaged EFG seen by the nucleus is effectively that of the static vacancy. This is the region below 240°K and corresponds, in the paramagnetic case, to the fully resolved Zeeman spectrum. In the fast motion situation the rapid movement of the vacancy results in the nucleus seeing a time-averaged EFG which is effectively zero (since the whole EFG is assumed to be a result of the presence of the vacancy). This occurs above 280°K and corresponds to the familiar single line situation in the paramagnetic case, e.g., Fe^{57} in stainless steel at all temperatures which have been examined.

In motional narrowing in NMR the criterion for the transition between fast and slow motion is that the Larmor precession time in the *perturbing field* be of the order of the fluctuation time of this field. Although the whole of the field at the nucleus, in our case, is time-

²² H. H. Wickman, Ph.D. thesis, University of California, Berkeley, 1964 (unpublished); I. Nowik and H. H. Wickman, Phys. Rev. **140**, A869 (1965); M. Blume, Phys. Rev. Letters **14**, 96 (1965).

²³ N. Bloembergen, E. M. Purcell, and R. V. Pound, Phys. Rev. **73**, 679 (1948); A. Abragam, *The Principles of Nuclear Magnetism* (Oxford University Press, New York, 1961), Chap. 10.

dependent we use this criterion to deduce a value of fluctuation time where the transition should occur. Translating to the case of a field gradient producing a quadrupole splitting $\Delta E(T)$ at temperature T , the criterion becomes $\Delta E(T)\tau_j/h \sim 1$; τ_j is the fluctuation time of the EFG, i.e., the jump time of the vacancy. Using Fig. 2, curve (b), to obtain $\Delta E(T)$ for a static vacancy, it is found that at 250°K the above criterion becomes $\tau_j \sim 3 \times 10^{-8}$ sec. To confirm that such jump times occur at these temperatures we have made dielectric dispersion measurements on both cobalt and iron-doped AgCl. These dispersions result from the finite orientation times of the vacancy-impurity dipoles. Watkins¹ has examined such effects for Mn^{++} ions in NaCl, and our experimental method and interpretation follows his closely except that our temperature range is lower. The dielectric loss of the sample was determined by a Boonton 160A Q-meter in the frequency range 200 kc/sec to 20 Mc/sec. The temperature of the sample in the coaxial holder could be held at values between 200 and 295°K.

The method has poor sensitivity due to the finite solubility of the impurities and the high dielectric constant of AgCl. However, plots of the logarithm of $\tan\delta$, where δ is the loss angle, versus \log frequency ω showed a linear dependence of slope -1 plus a superimposed peak (see Watkins¹). The linear term is due to the conductivity of the crystal and the peak is supposedly the effect of the vacancy-impurity pairs. At lower temperatures ($< 280^\circ\text{K}$) where the conductivity is small the vacancy-impurity pairs dominate. The peaks were found to be broader than expected from a single Debye-relaxation time. Figure 10 shows a plot of $\log\tau_r$ versus reciprocal absolute temperature where τ_r is the reciprocal of the frequency at the center of the loss peak and represents some average relaxation time. The points in Fig. 10 are for an iron-doped sample. The error bars give an estimation of the spread in relaxation times. The two open circles are taken from the work of Bottger²⁴ who measured $\tan\delta$ versus temperature at two frequencies for AgCl doped with transition metal impurities including cobalt. For each of the two frequencies he found a well defined maximum in $\tan\delta$ with these maxima occurring at temperatures which were effectively independent of the identity of the impurity. We have taken the reciprocal of his two frequencies and plotted them as relaxation times. As can be seen from Fig. 10 these results are consistent with ours if τ_r has the form $A \exp(E/kT)$. The line (a) represents the values $A = 1.5 \times 10^{-11}$ sec, $E = 0.35$ eV. This type of dependence of τ_r was found by Watkins for Mn^{++} in NaCl but with $A \sim 10^{-12}$ sec, $E \sim 0.63$ eV. His $\tan\delta$ peaks, however, could be fitted with a single relaxation time.

The line (b) in Fig. 10 represents the spin relaxation (vacancy jump) times for the AgCl: Mn^{++} system from the work of Daehler.² As expected these times are

²⁴ H. Bottger, Phys. Status Solidi 4, 669 (1964).

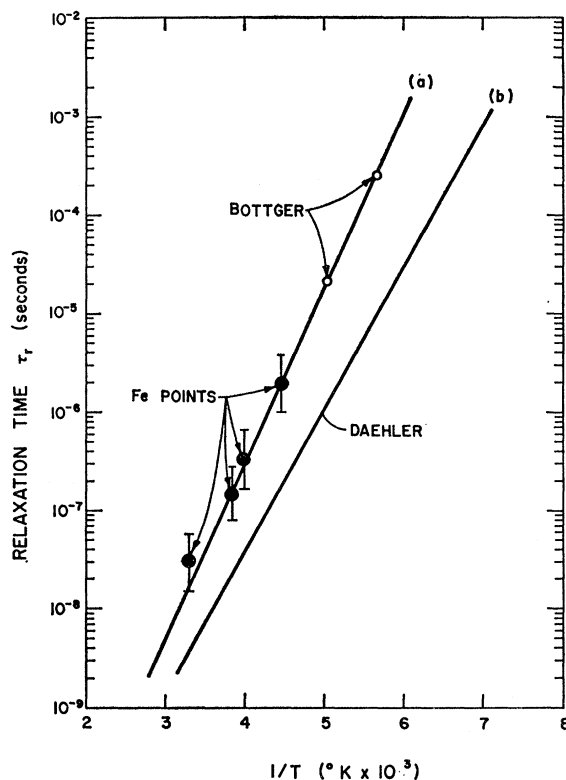


FIG. 10. Logarithm of the dielectric relaxation time τ_r versus reciprocal absolute temperature. The closed circles are points derived from the present experiment with an iron-doped AgCl crystal. The two open circles are from the work of Bottger (Ref. 24) and represent the dielectric dispersion of several transition ions in AgCl including cobalt. The line (a) represents the expression $\tau_r = A \exp(E/kT)$ with $A = 1.5 \times 10^{-11}$ sec and $E = 0.35$ eV. The line (b) illustrates the experimental results of Daehler for ESR relaxation times in the system AgCl: Mn^{++} (Ref. 2).

considerably shorter than the vacancy-impurity dipole orientation time. It is noted that the vacancy must make a minimum of four jumps to reorient a (100) dipole through 180° . If the factor given by Watkins relating τ_j and τ_r is taken as correct, i.e., $\tau_j = \tau_r/7$, we see from Fig. 10 that at 250°K, $\tau_j \sim 3 \times 10^{-7}/7 \sim 4 \times 10^{-8}$ sec, whereas Daehler finds $\sim 3 \times 10^{-8}$ sec. Thus the dielectric relaxation, ESR and Mössbauer effect are consistent with respect to the characteristic times of vacancy motion.

VII. IONIC CONDUCTIVITY

The interpretation of the spectrum collapse in Section V implies that the vacancy remains attached to the Fe^{++} and does not dissociate in the temperature range of interest (230–280°K). To test the validity of this assumption and also to determine the number of vacancies introduced per cobalt impurity, measurements of ionic conductivity have been made in the temperature range 300 to 700°K. Data was taken on both cobalt and iron-doped crystals using a 1000 c/sec ac bridge in the manner of Abbink.¹⁶ The con-

centrations of dopant were determined by emission analysis.

Using the known cation-vacancy mobility and intrinsic-defect concentrations from the careful work of Abbink¹⁵ and others,²⁵ the fraction of iron and cobalt ions bound to a vacancy at any temperature can be calculated. It is found that cobalt and iron give very similar conductivity curves. The results suggest single-vacancy binding energies⁹ in the range 0.2–0.3 eV. Roughly $\frac{1}{3}$ of the iron and cobalt ions at room temperature are dissociated from a vacancy. Using the measured binding energies it is found that less than 10% of the impurities are free at 280°K.

VIII. MODEL FOR SPECTRUM II

Spectrum II is thought to be a result of the binding of a doubly negatively charged impurity to a cobalt ion in place of the vacancy. Apparently the cobalt-impurity binding energy is larger than that for the cobalt-vacancy. Since the impurity is expected to be an anion and hence bound in a nearest neighbor (100) position this is hardly surprising. The slow growth rate of II is therefore due to the relatively slow movement of the impurity and cobalt through the lattice. Heating at 100°C and above leads to dissociation; the diffusion rates are too slow to follow the cooling rate and hence a nonequilibrium distribution is quenched-in. If this model is correct, an increase in the concentration of inactive cobalt in the dopant will inhibit the growth rate of II. It was found that an increase in concentration by a factor of 20 so decreased the growth rate that the intensity of II was still negligible after three weeks storage at room temperature. The opposite situation apparently occurs for the oxygen doped sample, where the anion concentration swamps that of the cobalt.

The differences in spectra II from sample to sample are probably due to different impurities, with possibly more than one present in one sample. The actual identities of the ions are not known, except for the oxygen case.

It is noted that the isomer shift of spectrum II is always near 0.08 cm/sec at room temperature. This is as close to 0.04 cm/sec, the value for a pure $3d^5$ state relative to iron, as to 0.125 cm/sec, the value for a $3d^6$ state, and possibly indicates a high measure of covalency in the binding.^{14,26}

IX. ΔE VERSUS T FOR SPECTRUM II

The symmetry of distortion is the same as in the case of the vacancy and the analysis of Sec. VB can be adopted for the present case. As might be expected ΔE is much larger than for spectrum I since B_2^0 , the axial crystalline field strength, is higher due to the proximity of the distorting charge.

²⁵ R. D. Foucheux and R. O. Simmons, Phys. Rev. **136**, A1664 (1964).

²⁶ N. L. Costa, J. Danon, and R. M. Xavier, J. Phys. Chem. Solids **23**, 1783 (1962).

Using Fig. 3 of Ref. 4 we obtain the curves shown in Fig. 5 with $\alpha^2=1$, $\Delta=230$ cm⁻¹. Although large errors are introduced by the analysis of the complex spectra, the theory can be seen to disagree with experiment. The fit cannot be improved by a decrease in α^2 , the covalency factor, as introduced for spectrum I since the experimental points lie above the theoretical ones. The small isomer shift, however, suggests that covalency is present to a greater degree than in spectrum I, hence α^2 would be expected to be markedly less than 1. It is possible that a crystalline-field symmetry other than axial would resolve this contradiction, e.g., Fig. 1 and Table II of Ref. 5.

X. f , δE

Since there is no theory for the Debye-Waller factor of an impurity in an ionic crystal, we note without comment that the plots of $\log f$ versus T in Fig. 6 are fitted by a Debye model in the high-temperature limit ($T > \Theta_D/2$),²⁷ with a Debye temperature of 150°K for the Spectrum I and the oxygen-doped sample and 130°K for spectrum II of Fig. 3(b). The specific-heat Debye temperature for AgCl is 183°K.²⁸ The spectrum I f values appear not to be strongly influenced by the presence of the vacancy, since the points at the temperatures where the Fe⁺⁺ is highly dissociated ($T > 400^\circ\text{K}$) lie on the same line as those of the lower temperatures.

It has been assumed that the anisotropic Debye-Waller factor leads to the observed difference in intensity of the two lines [Figs. 1(b) and (c)]. The fact that this difference increases with temperature is consistent with this view¹⁹; it is expected that the anisotropy will be such that the atom will have greater displacement in the direction of the vacancy: i.e., the recoilless fraction is a minimum in the (100) direction, the axis of EFG. From a consideration of the angular dependence of the intensity distributions of the transitions from the $\pm\frac{3}{2}$ and $\pm\frac{1}{2}$ states,²⁷ it can be seen that the line corresponding to the $\pm\frac{1}{2}$ transition is expected to be the more intense. Since in our model the EFG is positive the $\pm\frac{1}{2}$ state has the less energy and should lie nearer zero velocity. This is observed.

The lines drawn in Fig. 7 are for a Debye model in the high-temperature limit and are arranged to pass through the appropriate experimental points at 80°K.

XI. SUMMARY

The main features of our investigation emerge as:

- (a) Crystals of AgCl can be obtained in which all the cobalt impurity ions occupy substitutional sites and are bound to a positive ion vacancy in a unique position.
- (b) In AgCl Fe⁵⁷ produced by K capture from doubly

²⁷ A. J. F. Boyle and H. E. Hall, Rept. Progr. Phys. **25**, 441 (1962).

²⁸ F. Seitz, *Modern Theory of Solids* (McGraw-Hill Book Company, New York, 1940), p. 110.

charged Co^{57} is present as Fe^{++} only. This is to be contrasted with NaCl where both Fe^+ and Fe^{+++} are observed.²⁹

(c) There is a noticeable degree of covalency in the binding of Fe^{++} in AgCl.

(d) The effect of the variation in fluctuation time of an EFG have been observed for the first time in the Mössbauer effect.

(e) The silver-ion-vacancy jump times are much faster than those of alkali-ion vacancies in the alkali

²⁹ J. G. Mullen, Phys. Rev. 131, 1415 (1963).

halides (about 10^5 faster at room temperature). These jump times are apparently largely independent of the identity of impurity.

ACKNOWLEDGMENTS

The authors thank G. de Pasquali for his generous help in the preparation of sources and absorbers. They also gratefully acknowledge the help of M. A. Ball, M. Blume, C. Cevikus, H. Frauenfelder, R. L. Ingalls, B. Joesten, M. Levine, R. J. Maurer, R. O. Simmons, C. P. Slichter, and H. Stapleton.

Ising-Model Reformulation. III. Quadruplet Spin Averages

FRANK H. STILLINGER, JR.

Bell Telephone Laboratories, Murray Hill, New Jersey

(Received 24 November 1965)

A previously developed method for diagrammatic expansion of the Ising-model partition function and pair distribution function is applied to calculation of the field-free quadruplet spin averages $\langle \mu_1 \mu_2 \mu_3 \mu_4 \rangle$. The central four-vertex function Q generated by these averages is topologically analyzed in standard fashion in terms of an irreducible four-vertex quantity e . Several rigorously necessary conditions that must be satisfied by Q are listed. It is furthermore pointed out that the existence of a logarithmic specific-heat anomaly puts an additional constraint on quadruplet averages (which is verified in an Appendix by direct calculation on the Ising-Onsager two-dimensional square lattice). Upon making a simplifying functional assumption for Q , this latter quantity may be entirely determined above T_c by one of the necessary conditions. This leads at T_c to a $k^{d/2}$ spectrum (d =dimensionality) and above T_c to a logarithmic specific heat, both of which were adduced by Abe's Ising-model version of the He⁴ speculative analysis due to Patashinskii and Pokrovskii (but for different reasons from those in the present analysis). Since the Abe-Patashinskii-Pokrovskii spectrum almost certainly exhibits an incorrect exponent, an alternative and more powerful functional assumption for Q is suggested which still yields a soluble theory in principle, but construction of the solution is not attempted here.

I. INTRODUCTION

IN a previous article,¹ some of the techniques of quantum field theory were employed to generate a diagram expansion for the general Ising-model partition function $Z(\beta)$ and low-order spin averages. The partition function was expressed as a vacuum-state expectation value of the product of two operators:

$$Z(\beta) = \langle 0 | \exp(-\beta \mathbf{M}) \exp(\mathbf{D}^\dagger) | 0 \rangle, \quad \beta = (k_B T)^{-1}, \quad (1)$$

and the "vacuum" may be regarded as a set of unexcited one-dimensional harmonic oscillators, one at each lattice site. Operators \mathbf{M} and \mathbf{D}^\dagger can be expressed in terms of the canonical boson field operators $\mathbf{b}(\mathbf{k})$ and $\mathbf{b}^\dagger(\mathbf{k})$:

$$\mathbf{M} = \sum_{\mathbf{k}}^{(\tau)} \{ H(-\mathbf{k}) \mathbf{b}^\dagger(\mathbf{k}) + H(\mathbf{k}) \mathbf{b}(\mathbf{k}) + V(\mathbf{k}) [\frac{1}{2} \mathbf{b}^\dagger(\mathbf{k}) \mathbf{b}^\dagger(-\mathbf{k}) + \mathbf{b}^\dagger(\mathbf{k}) \mathbf{b}(\mathbf{k}) + \frac{1}{2} \mathbf{b}(\mathbf{k}) \mathbf{b}(-\mathbf{k})] \}; \quad (2)$$

¹ F. H. Stillinger, Jr., Phys. Rev. 135, A1646 (1964).

$$\mathbf{D}^\dagger = \sum_{n=2}^{\infty} N^{1-n} D_n \sum_{\mathbf{k}_1 \cdots \mathbf{k}_{2n-1}}^{(\tau)} \mathbf{b}^\dagger(\mathbf{k}_1) \cdots \mathbf{b}^\dagger(\mathbf{k}_{2n-1}) \times \mathbf{b}^\dagger(-\mathbf{k}_1 - \cdots - \mathbf{k}_{2n-1}). \quad (3)$$

Here, $H(\mathbf{k})$ and $V(\mathbf{k})$ are the discrete-lattice Fourier transforms of the external field $h(\mathbf{r})$ and the pair potential $v(\mathbf{r})$, and the \mathbf{k} 's are the reciprocal lattice vectors, confined to the first Brillouin zone τ . The numerical coefficients D_n may be expressed as the following integrals:

$$D_n = \frac{(-1)^{n-1} 2^{2n}}{\pi^{2n} (2n)!} \int_0^\infty \frac{y^{2n-1} dy}{\sinh y}, \quad (4)$$

or alternatively written in terms of Bernoulli numbers.

In Ref. 1 it was convenient to consider the operators $\exp(\mathbf{D}^\dagger)$ and $\exp(-\beta \mathbf{M})$ in Eq. (1) to act, respectively, during "time" intervals of unit length and length β . Time ordering of operators, followed by operator contractions in accord with Wick's theorem then generated the requisite diagrams.